

Role of a Cluster of Hydrophobic Residues Near the FAD Cofactor in *Anabaena* PCC 7119 Ferredoxin-NADP⁺ Reductase for Optimal Complex Formation and Electron Transfer to Ferredoxin*

Received for publication, March 8, 2001, and in revised form, May 4, 2001
Published, JBC Papers in Press, May 7, 2001, DOI 10.1074/jbc.M102112200

Marta Martínez-Júlvez‡, Isabel Nogués‡, Merche Faro‡, John K. Hurley§, Tammy B. Brodie§, Tomás Mayoral¶, Julia Sanz-Aparicio¶, Juan A. Hermoso¶, Marian T. Stankovich||, Milagros Medina‡, Gordon Tollin§, and Carlos Gómez-Moreno‡**

From the ‡Departamento de Bioquímica y Biología Molecular y Celular, Facultad de Ciencias, Universidad de Zaragoza, 50009-Zaragoza, Spain, the §Department of Biochemistry and Molecular Biophysics, University of Arizona, Tucson, Arizona 85721, ¶Grupo de Cristalografía Macromolecular y Biología Estructural, Instituto Química-Física Rocasolano, C.S.I.C. Serrano 119, 28006-Madrid, Spain, and the ||Department of Chemistry, University of Minnesota, Minneapolis, Minnesota 55455

In the ferredoxin-NADP⁺ reductase (FNR)/ferredoxin (Fd) system, an aromatic amino acid residue on the surface of *Anabaena* Fd, Phe-65, has been shown to be essential for the electron transfer (ET) reaction. We have investigated further the role of hydrophobic interactions in complex stabilization and ET between these proteins by replacing three hydrophobic residues, Leu-76, Leu-78, and Val-136, situated on the FNR surface in the vicinity of its FAD cofactor. Whereas neither the ability of FNR to accept electrons from NADPH nor its structure appears to be affected by the introduced mutations, different behaviors with Fd are observed. Thus, the ET interaction with Fd is almost completely lost upon introduction of negatively charged side chains. In contrast, only subtle changes are observed upon conservative replacement. Introduction of Ser residues produces relatively sizable alterations of the FAD redox potential, which can explain the modified behavior of these mutants. The introduction of bulky aromatic side chains appears to produce rearrangements of the side chains at the FNR/Fd interaction surface. Thus, subtle changes in the hydrophobic patch influence the rates of ET to and from Fd by altering the binding constants and the FAD redox potentials, indicating that these residues are especially important in the binding and orientation of Fd for efficient ET. These results are consistent with the structure reported for the *Anabaena* FNR:Fd complex.

There are many examples throughout biology in which physiological function involves protein-protein interaction. Important illustrations of this are the reactions that occur between

proteins in the ET¹ chains participating in photosynthesis, respiration, nitrogen fixation, and cytochrome P450 hydroxylations. In all of these cases, specific recognition and binding occur between the donor and the acceptor proteins. Although the structural parameters that determine such recognition are not fully understood, it is widely accepted that a transient complex between the two proteins must be formed and that the mutual orientation of the two proteins within the complex determines the rate of the ET reaction. For the last 10 years a large effort has gone into the study of the interaction between two ET proteins participating in the metabolism of the cyanobacterium *Anabaena* PCC 7119, ferredoxin (Fd), and ferredoxin-NADP⁺ reductase (FNR) (1–18). During photosynthesis, FNR catalyzes the transfer of electrons from the one-electron carrier Fd to the two-electron acceptor NADP⁺ to produce NADPH (19). Both proteins from *Anabaena* have been cloned and expressed in *Escherichia coli* (20–22), and their high resolution x-ray structures have been determined (23, 24). All of the biochemical and structural information available on these proteins indicates that Fd binds in a concave cavity around the FAD group of the reductase (2, 25), and this hypothesis has been strongly supported by the recent x-ray structures reported for the complex formed by Fd and FNR, either with the *Anabaena* or the maize leaf proteins (26, 27).

During the last 2 decades different approaches have been used to investigate the involvement of electrostatic interactions in complex formation and ET between FNR and Fd (1, 2, 6–10, 12, 13, 15–17, 28). The reported data confirm the importance of such electrostatic interactions, provided mainly by negatively charged residues on the Fd surface and positively charged residues on FNR, in complex formation, and in the reorientation of FNR and Fd in order for an efficient ET process to occur. Despite this, charge-reversal mutations at most of the positively charged residues on *Anabaena* FNR situated at the putative interaction surface, such as Arg-16, Lys-72, Lys-138, Arg-264, Lys-290, or Lys-294, produce only moderate to no impairment of complex formation and ET with Fd (10, 17). Thus, only two charged residues on the FNR surface appear to have a crucial role in these processes. One is the Lys residue at position 75 of the *Anabaena* protein, which has been clearly

* This work was supported by Grant BIO97-0912C02-01 of Comisión Interministerial de Ciencia y Tecnología (to C. G.-M.) and by Grant DK15057 from the National Institutes of Health (to G. T.). The costs of publication of this article were defrayed in part by the payment of page charges. This article must therefore be hereby marked "advertisement" in accordance with 18 U.S.C. Section 1734 solely to indicate this fact.

The atomic coordinates and structure factors (code 1qgz, 1qh0, and 1h85) have been deposited in the Protein Data Bank, Research Collaboratory for Structural Bioinformatics, Rutgers University, New Brunswick, NJ (<http://www.rcsb.org/>).

** To whom correspondence should be addressed: Dept. de Bioquímica y Biología Molecular y Celular, Facultad de Ciencias, Universidad de Zaragoza, 50009-Zaragoza, Spain. Tel.: 34 976 761288; Fax: 34 976 762123; E-mail: gomez@posta.unizar.es.

¹ The abbreviations used are: ET, electron transfer; DCPIP, 2,6-dichlorophenol-indophenol; dRf, 5-deazariboflavin; dRfH[•], dRf semiquinone radical; Fd, ferredoxin; FNR, ferredoxin-NADP⁺ reductase; Fd_{ox}, Fd in oxidized state; Fd_{red}, ferredoxin in reduced state; FNR_{red}, FNR in reduced state; WT, wild type; MES, 4-morpholineethanesulfonic acid.

A

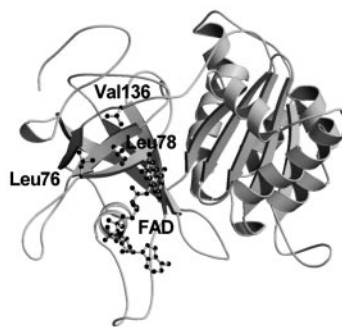


FIG. 1. A, Molscript (54) representation of *Anabaena* WT FNR showing the mutated residues in a ball and sticks representation. The FAD cofactor is also shown. B, sequence alignment of different members of the FNR family in the regions containing the Leu-76, Leu-78, and Val-136 residues of *Anabaena* FNR. Hyphens denote gaps introduced to improve alignment.

B

FNR species	76 78	136
<i>Anabaena</i> PCC 7119	PEKLRLYSIAS [*] TRHGDDVDDKT	SEVKIT-GPVGKEML [20]
<i>Spirulina</i> sp	PHKLRLYSIAS [*] TRHGDDVDDKT	ADVAIT-GPVGKEML [56]
Spinach (leaf)	PHKLRLYSIASSALGDFGDAKS	AEVKLT-GPVGKEML [57]
Pea (leaf)	PHKLRLYSIASSAIGDFGDSKT	SEVKIT-GPVGKEML [58]
Pea (root)	PHNVRLYSIAS [*] TRYGDNFDGKT	DKIKIA-GPSGKIML [59]
Rice (leaf)	PHKLRLYSIASSALGDFGDSKT	SDVKIT-GPVGKEML [60]
Tobacco (leaf)	PHKLRLYSTASSALGDFGDSKT	AEVKIT-GPVGKEML [61]
Tobacco (root)	PHNVRVLIAS [*] TRYGDSFDGKT	DKVKIT-GPSGKIML [62]
FNR-LIKE PROTEINS		
CYP450R, rat	RLQARYYSIASSSKVH---PNS	ALVPMF-VRK-SQFR [63]
NOS, human	LLQPRYSISSSPDMY---PDE	ELVPCFVRGAPS-FH [64]
SiR, <i>E. coli</i>	PLTPRLYSIASSQA----EVEN	EGEVRFVIEHNDNFR [65]
NR, corn (leaf)	KLCMRAYTPTSMVD----EIGH	SYIDVK-GPLGHV-E [66]
NR, corn (root)	KLCMRAYTPTSPVD----EVGH	ATIDIK-GPHRHI-E [67]
Cb5R, human	NLVVRPYTPISSDD----DKGF	DTIEFR-GPSGLL-V [68]
Cb5R, pig	NLVIRPYTPVSSDD----DKGF	DTIEFR-GPNGLL-V [69]
PDR, <i>P. Cepacia</i>	-GSRRTYSLCNSQE----RNR	DAVEVS-LPR-NEFP [70]

established to require a positively charged side chain for complex formation with its physiological protein partners to produce ET (15). The other crucial charged residue on FNR, Glu-301, is neither positively charged nor is it involved in complex formation but has been clearly shown to be a critical residue for ET to the FNR protein partners (14, 29). Similar results have been reported for charge-reversal mutations on the Fd surface. Thus, it has been shown that charge-reversal mutations of acidic residues such as Asp-62, Asp-67, Asp-68, Asp-69, or Glu-95 have either a moderate or no effect on complex stability and ET with the reductase (4). In contrast, a charge-reversal mutation of Glu-94 has large effects on the ET reactivity (4, 6, 9). The crucial role of Glu-94 has been discussed in terms of the Fd x-ray structure. It has been shown that this residue forms a hydrogen bond with the hydroxyl group of Ser-47, which has also been shown to be a critical residue, suggesting an important role of these two residues in the stabilization of the molecular surface of the Fd. It is noteworthy that the critical function played by Glu-94 cannot be carried out by an adjacent residue in the sequence, which is also a Glu residue, Glu-95, indicating the importance of the geometry and the specific nature of the interaction between FNR and Fd. These mutagenesis results are supported by the previously mentioned crystallographic structure of the *Anabaena* FNR-Fd complex, where it has been shown that Fd Glu-94 is involved in a well defined hydrogen bond with Lys-75 of FNR and that no other charged residues in either of the proteins are directly involved in the interaction surface (26).

Recent studies have shown that other types of interactions, e.g. hydrophobic interactions, might be stronger than electrostatic forces at protein-protein interfaces (30–33) and might

play a more active role in complex formation, as has been described for systems such as hormone-receptor or antigen-antibody complexes (34, 35). In the FNR/Fd system, previous studies have indicated that an aromatic amino acid residue on the surface of Fd, Phe-65, was essential for the efficient ET reaction between Fd and FNR (5). Moreover, thermodynamic and kinetic analyses of this system have suggested that hydrophobic interactions, which seem to originate from the dehydration of the protein-protein interface (3, 7), play an important role. In the present study we further investigate the role of hydrophobic interactions in complex stabilization and ET between Fd and FNR, by analyzing the function of several hydrophobic residues that the three-dimensional structure of the protein shows are situated on the protein surface in the vicinity of the FAD isoalloxazine ring (Fig. 1A). These amino acids, Leu-76, Leu-78, and Val-136 of *Anabaena* FNR, are fully conserved in all photosynthetic FNRs from different species (Fig. 1B). In this study we have replaced these residues by a series of amino acids in order to establish their involvement and to assess the importance of hydrophobic interactions in the processes of complex formation and ET in the FNR/Fd system. Our results clearly indicate that these residues are important for efficient ET and provide additional evidence that the crystallographic structure reported for the *Anabaena* FNR-Fd complex (26) represents a viable model for a productive ET complex.

EXPERIMENTAL PROCEDURES

Oligonucleotide-directed Mutagenesis—The FNR mutants were produced using a construct of the *petH* gene, which had been previously cloned into the expression vector pTrc99a, as a template (20). The MORPH mutagenesis kit (5 Prime → 3 Prime, Inc., Boulder, CO) was used to prepare the L76A, L78A, L76V, L78V, L76F, L78F, L76F/L78F,

L76S, L78S, V136S, and V136A mutants. The L76D, L78D, V136L, and L76D/L78D substitutions were obtained using the Transformer site-directed mutagenesis kit from CLONTECH (Palo Alto, CA) as has been described previously (15). Mutations were verified by DNA sequence analysis. The constructs containing the mutated FNR gene were used to transform the *E. coli* PC 0225 strain.

Purification of the Fd, FNR, and FNR Mutants—FNR mutants were purified from isopropyl- β -D-thiogalactoside-induced LB cultures, as described previously (14). Recombinant wild-type Fd from *Anabaena* was prepared as described (4). UV-visible spectra and SDS-polyacrylamide gel electrophoresis were used as purity criteria.

Spectral Analysis—UV-visible analyses were carried out using a KONTRON Uvikon 942, an OLIS (Bogart, GA) modified Cary-15, or Varian Cary-300 spectrophotometer. Dissociation constants, binding energies, and extinction coefficients of the complexes between oxidized FNR species and oxidized ferredoxin were measured by differential absorption spectroscopy as described previously (14). These experiments were performed on solutions containing $\sim 20 \mu\text{M}$ FNR in 50 mM Tris/HCl buffer, pH 8.0, at 25 °C. Aliquots of concentrated Fd were titrated into this solution. Circular dichroism was carried out on a Jasco 710 spectropolarimeter at room temperature in a 1-cm path length cuvette in 1 mM Tris/HCl buffer, pH 8.0. The protein concentrations were 0.7 μM for the far-UV and 4 μM for the aromatic and visible region of the spectrum.

Enzymatic Assays—The diaphorase activity was assayed with DCPIP as artificial electron acceptor, and the FNR-dependent NADPH-cytochrome *c* reductase activity using Fd as electron acceptor was determined in order to establish the steady-state kinetic parameters for the different FNR mutants (14).

Laser Flash Photolysis Measurements—The laser flash photolysis system was as described previously (36), except that a Tektronix TDS 410A digitizing oscilloscope was employed in the present system. The photochemical system that generates reduced protein *in situ* has also been described (37). Briefly, the laser pulse excites 5-deazariboflavin (dRf) to the triplet state which abstracts a hydrogen atom from EDTA to form the highly reducing dRf semiquinone radical (dRf \cdot). In competition with its own disproportionation, dRf \cdot reduces Fd $_{\text{ox}}$ present in the sample. Kinetic experiments were performed under pseudo first-order conditions in which Fd $_{\text{ox}}$ is present in large excess over the concentration of dRf \cdot generated by the laser flash ($< 1 \mu\text{M}$). Samples containing 0.1 mM dRf and 1 mM EDTA in 4 mM potassium phosphate buffer, pH 7.0, were deaerated in a long stem 1-cm path length cuvette by bubbling with H $_2$ O-saturated argon gas for 1 h. Microliter volumes of concentrated protein were introduced through a rubber septum using a Hamilton syringe. When necessary, argon gas was blown over the sample surface to remove traces of added O $_2$. Generally, 4–10 flashes were averaged. Kinetic traces were analyzed using a computer fitting routine (Kinfit, OLIS, Bogart, GA). Experiments were performed at room temperature.

Stopped-flow Kinetics Measurements—ET processes between FNR and Fd were studied by stopped-flow methodology under anaerobic conditions using an Applied Photophysics SX17.MV spectrophotometer interfaced with an Acorn 5000 computer using the SX.18MV software of Applied Photophysics as described previously (14). All samples were made anaerobic by successive evacuation and flushing with O $_2$ -free argon before introduction into the stopped-flow syringes. Samples of reduced Fd and FNR were prepared by photoreduction of the protein-bound redox center in 50 mM Tris/HCl, pH 8.0, also containing 20 μM EDTA and 2–4 μM dRf. Reactions were performed at 13 °C. The observed rate constants (k_{obs}) were calculated by fitting the data to a mono- or biexponential equation. The measurement of the reoxidation rate of FNR $_{\text{red}}$ by molecular oxygen was carried out on a solution of air-saturated 50 mM Tris/HCl, pH 8.0.

Midpoint Redox Potential Measurements—Potentiometric titrations of recombinant WT and L76S, L76D, L76F, L78S, L78D, L78F, L76D/L78D, and V136S mutants of *Anabaena* FNR were performed using a three-electrode electrochemical cell (38). Typical experimental solutions contained 12–20 μM protein, 1–3 μM indicator dyes, 1 μM dRf, 1 mM EDTA, and 10% (by volume) glycerol (included to prevent the appearance of turbidity) in 50 mM Tris/HCl buffer, pH 8.0, at 10 °C. Indicator dyes were selected to cover the experimental potential range of each protein titration. These included lumiflavin 3-acetate (–223 mV), benzyl viologen (–348 mV), and methyl viologen (–443 mV). The dRf and EDTA were present to initiate photoreduction of proteins via the highly reductive deazaflavin radical (39). Alternative reduction methods such as electrochemical mediation by methyl viologen yielded similar results. Experimental solutions were made anaerobic through several cycles of argon introduction and removal by vacuum over a total period

of 2 h. Stepwise photoreduction of proteins was achieved by irradiating the solution (with the cell immersed in ice water) with a 650-watt projector bulb for ~ 1 min per titration point. After reduction, the cell was placed in a temperature-controlled holder in a PerkinElmer Life Sciences 2S spectrophotometer interfaced with an IBM-compatible computer. The solution potential was monitored using an Orion Research model 601A digital ion analyzer. Equilibration of the system was considered established when the measured potential remained stable for 10 min; the UV-visible spectrum was then measured. Prior to redox species quantitation, turbidity and dye contributions were subtracted. Upon reoxidation by air at the end of each experiment, $>95\%$ of the protein was recovered. The FAD semiquinone is not very stable in this protein; during the titrations the proportion of the total FAD in the form of the semiquinone at equilibrium was very low, and it was not possible to measure the redox potentials for the two one-electron steps directly. Therefore, values for the midpoints potentials (E_m) of the two-electron reduction of the enzyme were calculated by linear regression analysis of plots of system potential *versus* logarithm of concentration ratio ($[\text{ox}]/[\text{red}]$) according to the Nernst Equation 1,

$$E = E_m + (0.056/n)\log([\text{ox}]/[\text{red}]) \quad (\text{Eq. 1})$$

where E is the measured equilibrium potential at each point in the titration; n is the number of electrons transferred to the system, and ($[\text{ox}]/[\text{red}]$) is the ratio between the redox species at equilibrium, as determined from the absorbance spectrum. Each FNR displayed Nernstian behavior based on the slopes of their Nernst plots (close to 28 mV, the theoretical slope for a two ET at 10 °C). All potentials in this study are reported *versus* the standard hydrogen electrode.

Crystal Growth, Data Collection, and Structure Refinement—Crystals from L78D, L76D/L78D, and V136L FNR mutants were grown by the hanging drop method. The 5-ml droplets consisted of 2 ml of 0.75 mM protein solution buffered with 10 mM Tris/HCl, pH 8.0, 1 ml of unbuffered β -octyl glucoside at 5% (w/v), and 2 ml of reservoir solution containing 18–20% (w/v) polyethylene glycol 6000, 20 mM ammonium sulfate, 0.1 M MES/NaOH, pH 5.0. The droplets were equilibrated against 1 ml of reservoir solution at 20 °C. Under these conditions crystals grew to a maximum size of about 0.6 \times 0.4 \times 0.4 mm within 1–7 days in the presence of phase separation caused by the detergent. Crystals of the L78D and V136L FNR mutant proteins were mounted in glass capillaries, and x-ray data were collected to a maximum resolution of 2.3 Å at 20 °C on a Mar Research (Germany) IP area detector using graphite monochromated CuK $_{\alpha}$ radiation generated by an Enraf-Nonius rotating anode generator. Synchrotron diffraction data were collected from frozen crystals at 100 K of the L76D/L78D FNR mutant on Beamline D2AM at ESRF (Grenoble). Crystals belong to the P6 $_5$ hexagonal space group, and the V_m is 3.0 Å 3 /Da with one FNR molecule in the asymmetric unit and 60% solvent content. All data sets were processed with MOSFLM (40) and scaled and reduced with SCALA from the CCP4 package (41). All the structures were solved by molecular replacement using the program AmoRe (42) on the basis of the 1.8-Å resolution native FNR model (24) without the FAD cofactor. An unambiguous single solution for the rotation and translation functions was obtained for all proteins. These solutions were refined by the fast rigid body refinement program FITING (43). The models were subjected to alternate cycles of conjugate gradient refinement with the program X-PLOR (44) and manual model building with the software package O (45). Finally, water molecules were added. The resulting model was again subjected to more cycles of positional and B-factor refinement. The final models consist of residues 9–303 (the first 8 residues were not observed in the electron density map), one FAD moiety, one SO $_4^-$ molecule, and solvent molecules. Relevant data collection statistics and refinement parameters are presented in Table I. The atomic coordinates for all mutants have been deposited in the Protein Data Bank with accession codes 1qgz for the L78D model, 1qh0 for the L76D/L78D, and 1h85 for the V136L.

RESULTS

Expression and Purification of the Different FNR Mutants—Mutants of FNR at positions Leu-76, Leu-78, and Val-136 were purified using the procedure described for the WT protein. In all cases the level of expression as well as the spectral properties were similar to those of the WT FNR (data not shown). This is taken as an indication that no major structural perturbations have been produced by the mutations.

Steady-state Kinetics of the FNR Mutants—The steady-state

TABLE I
X-ray data

Data collection	L78D	L76D/L78D	V136L
Temperature (K)	291	100	291
X-ray source	Rotating anode	Synchrotron	Rotating anode
Space group	P6 ₅	P6 ₅	P6 ₅
Cell a, b, c (Å)	88.03; 88.03; 97.26	86.94; 86.94; 96.59	86.65; 86.65; 96.56
Resolution range (Å)	35.6 – 2.3	35.1 – 1.9	37.5 – 2.3
No. of unique reflections	18,686	28,625	18,325
Completeness of data (%)			
All data	99.4	92.0	99.4
Outer shell	96.0	58.0	96.4
R_{sym}^a (%)	8.1	8.9	9.9
Refinement statistics	L78D	L76D/L78D	V136L
Resolution range (Å)	7.0 – 2.3	7.0 – 1.9	10.0 – 2.3
No. of protein atoms	2338	2338	2339
No. of heterogen atoms	58	58	58
No. of solvent atoms	268	481	314
R_{factor}^b (%)	17.8%	21.0%	20.9%
Free R_{factor} (%)	22.7%	25.0%	26.4%
Root mean square deviation			
Bond lengths (Å)	0.007	0.007	0.011
Bond angles (degree)	1.19	0.91	0.95

$$^a R_{\text{sym}} = \frac{\sum_{hkl} \sum_i |I_i - \langle I \rangle|}{\sum_{hkl} \sum_i I_i}$$

$$^b R_{\text{factor}} = \frac{\sum \|F_o\| - |F_c|}{\sum \|F_o\|}$$

kinetic parameters of the different FNR mutants were determined in two different enzymatic assays. The FNR diaphorase activity, measured with DCPIP as electron acceptor, can be taken as a measure of the ability of the enzyme to be reduced by the pyridine nucleotide, which acts as electron donor. The values obtained in this assay for k_{cat} , K_m for NADPH, and k_{cat}/K_m for the different FNR mutants are reported in Table II, showing three slightly different behaviors. Thus, L76A, L76V, L76F, L76S, L78S, L76F/L78F, V136L, and V136S had k_{cat} values in a range of 0.6–1.3 times that of the WT enzyme. The k_{cat} values determined for L78V and L78F were 1.8-fold larger than that of the WT and that of L78A was increased 3.7-fold, indicating a slightly more efficient ET process. Finally, the k_{cat} values for L76D, L78D, L76D/L78D, and V136A were smaller than that of the WT by 3-fold, demonstrating a less efficient ET process for these mutants. The K_m values of all the mutants were within a factor of 1.5 of that of the WT, with the exception of L78A, L76F/L78F, and V136A whose K_m values for NADPH were up to 3.5-fold larger. This can be taken as an indication that for most of the mutations, the ability of the protein to interact with NADPH has not been altered. However, the introduction of an Ala at positions 78 or 136 or the simultaneous replacement of Leu 76 and 78 by Phe might decrease the stability of the complex formed between the reductase and the pyridine nucleotide. Thus, only the introduction of negatively charged residues at positions 76 or 78 or the replacement of Val-136 by Ala produces enzymes that are up to 9-fold less efficient than the WT enzyme in the diaphorase assay. Moreover, it is noteworthy that the introduction of single Phe residues at positions 76 or 78, or a Val at position 78, produces a slight increase in the efficiency of the mutated enzymes in the assay (up to 2.5-fold).

The NADPH-dependent cytochrome *c* reductase activity of the FNR enzyme was also assayed using Fd as electron acceptor for the different FNR mutants at positions Leu-76, Leu-78, and Val-136 (Table II). This assay is affected not only by the interaction of NADPH with the enzyme but also by the interaction of the ET protein with the reductase. Important differences were observed for the kinetic parameters of some mutants relative to those of the WT. Thus, only V136L exhibited a higher k_{cat} value, although just slightly, whereas L76A, L76S, L76F, L78V, L78F, V136A, and V136S had k_{cat} values that were decreased by 50% or less relative to the WT enzyme. The

k_{cat} values obtained for the other FNR mutants were less than 25% that of the WT. Particularly noticeable are the low k_{cat} values obtained upon the introduction of negative charges at positions 76 or 78, with the reaction being almost totally inhibited if such negative charges were introduced simultaneously at both positions. The low k_{cat} values observed for L78S and the double mutant L76F/L78F are also remarkable. The K_m values for Fd obtained for most of the mutants are within a factor of 2 of that determined for the WT, whereas L76S and L78F show moderate increases in K_m , 3.5- and 5.5-fold, respectively. However, the corresponding values for L76D and L78D are much larger indicating that the introduction of a negatively charged residue at these positions strongly affects the interaction between FNR and Fd. By taking these values into account, as well as those of the diaphorase activity, it is clear why most of the mutants have lower catalytic efficiencies in this assay than the WT enzyme, having catalytic efficiencies that are 20–100% that of WT FNR (Table II). Most noteworthy is the very low efficiency, or even lack of reaction, exhibited in this assay by L76D, L78D, and L76D/L78D, which may be principally due to the formation of a very weak complex with Fd (Table III; see below). It should be pointed out that the lowered efficiency of this process could also be due in part to a low efficiency for the reaction between NADPH and FNR. Considerably diminished catalytic efficiencies were also observed for L78F and L76F/L78F. Surprisingly, the data indicate different reasons for such low values. Thus, whereas the lower catalytic efficiency of L78F seems to be due to weaker complex formation with Fd, this property does not appear to be affected for the double mutant, L76F/L78F. In the latter case it is the ET process itself that appears to be affected.

Interaction of FNR Forms with Fd—To determine further whether the introduced mutations affected Fd binding to FNR, difference absorption spectroscopy was used to evaluate directly the dissociation constants and binding energies for the complexes formed between the different FNR_{ox} mutants and Fd_{ox} (Fig. 2). When Fd_{ox} binds to WT FNR_{ox} the visible spectrum of the bound flavin undergoes a perturbation, yielding the difference spectrum shown in Fig. 2A (46). This has been proposed to be due to the alteration of the environment of the flavin ring due to Fd binding. Such spectral perturbations were

TABLE II
Steady-state kinetic parameters of wild-type and mutated FNR forms from *Anabaena*

FNR	Diaphorase activity			NADPH-dependent cytochrome <i>c</i> reductase activity ^a		
	k_{cat} s^{-1}	K_m^{NADPH} μM	$k_{\text{cat}}/K_m^{\text{NADPH}}$ $\mu\text{M}^{-1} s^{-1}$	k_{cat} s^{-1}	K_m^{Fd} μM	$k_{\text{cat}}/K_m^{\text{Fd}}$ $\mu\text{M}^{-1} s^{-1}$
WT ^b	81.5 ± 3.0	6.0 ± 0.6	13.5 ± 0.5	225 ± 3	23.0 ± 1.2	9.8 ± 0.2
L76A	51.3 ± 0.5	6.1 ± 0.3	8.4 ± 0.3	136 ± 10	36 ± 5	3.8 ± 0.8
L76D	24 ± 8	3.9 ± 1.2	6.1 ± 0.1	30.4 ± 1.2	>500	<0.06
L76V	61.6 ± 0.5	3.9 ± 0.3	17.3 ± 1.3	48.1 ± 4.7	14.0 ± 0.1	3.4 ± 0.3
L76F	108 ± 1	4.4 ± 0.2	24.3 ± 0.6	98 ± 2	28.4 ± 0.3	3.5 ± 0.8
L76S	68 ± 9	5.1 ± 0.9	13.6 ± 0.6	151 ± 40	81 ± 7	1.9 ± 0.6
L78A	303 ± 33	21.4 ± 0.2	14.1 ± 1.4	50.0 ± 2.5	8.3 ± 1.0	6.0 ± 0.3
L78D	24 ± 11	7.2 ± 1.1	3.3 ± 1.0	10.6 ± 5.4	>500	<0.02
L78V	147 ± 8	6.1 ± 0.1	23.8 ± 1.8	183 ± 19	21.3 ± 1.4	8.7 ± 1.5
L78F	138 ± 4	4.1 ± 0.2	33.9 ± 0.9	160 ± 7	127 ± 10	1.3 ± 0.2
L78S	100 ± 10	7.9 ± 1.1	12.5 ± 0.5	28.8 ± 0.1	14.3 ± 2.6	2.1 ± 0.3
L76D/L78D	33.8 ± 1.8	3.1 ± 0.4	11.0 ± 0.5	ND ^c	ND ^c	ND ^c
L76F/L78F	93 ± 6	15 ± 1	6.1 ± 0.1	11.4 ± 0.3	18.3 ± 1.4	0.6 ± 0.1
V136A	29.6 ± 4.3	19.5 ± 3.0	1.5 ± 0.1	105 ± 5	36.2 ± 3.2	2.5 ± 0.2
V136L	88 ± 3	3.9 ± 0.6	22.6 ± 0.3	261 ± 22	46 ± 6	5.7 ± 0.3
V136S	72 ± 2	7.0 ± 0.5	10.3 ± 0.6	116 ± 10	42 ± 4	2.7 ± 0.2

^a NADPH was present at saturating concentration when determining the K_m for Fd.

^b Data from Ref. 14.

^c No reaction was detected.

TABLE III

Dissociation constants and free energies for complex formation of oxidized wild-type and mutated *Anabaena* PCC 7119 FNR forms with oxidized ferredoxin

All of the difference spectra were recorded in 50 mM Tris/HCl, pH 8.0, at 25 °C. All of the proteins were in the oxidized state. ND, not determined.

FNR form	K_d μM	$\Delta\epsilon$ (462 nm) $\text{mM}^{-1} \text{cm}^{-1}$	ΔG^0 kcal mol^{-1}
WT	4.0 ± 1.0	2.0 ± 0.1	-7.3 ± 0.2
L76A	1.3 ± 0.2	1.8 ± 0.1	-8.0 ± 0.1
L76D ^a	ND	ND	ND
L76V	3.3 ± 1.1	1.1 ± 0.1	-7.4 ± 0.2
L76F	7.6 ± 4.7	2.6 ± 0.4	-7.0 ± 0.2
L76S	11.0 ± 2.6	0.8 ± 0.1	-6.7 ± 0.1
L78A	10.4 ± 4.8	2.7 ± 0.4	-6.8 ± 0.2
L78D ^a	ND	ND	ND
L78V	2.9 ± 0.8	2.4 ± 0.1	-7.5 ± 0.2
L78F	27.4 ± 10.4	1.5 ± 0.2	-6.2 ± 0.2
L78S	6.3 ± 2.5	0.36 ± 0.02	-7.1 ± 0.2
L76D/L78D ^a	ND	ND	ND
L76F/L78F ^b	16.2 ± 5.9	0.74 ± 0.06	-6.5 ± 0.1
V136A	2.2 ± 1.1	2.3 ± 0.1	-7.7 ± 0.2
V136L	5.4 ± 1.6	1.6 ± 0.1	-7.2 ± 0.1
V136S	3.3 ± 1.4	0.43 ± 0.02	-7.4 ± 0.2

^a Spectral perturbation was not detected.

^b Spectral perturbations were followed at 390 nm for these determinations.

detected for all the FNR mutants studied here upon Fd_{ox} addition (Fig. 2), with the only exceptions being the L76D, L78D, and L76D/L78D FNR forms for which no differences were detected in the flavin region of the spectra. These latter data confirm that the introduction of a negative charge at positions 76 or 78 completely eliminates the ability of the enzyme to form a stable complex with Fd. For the other mutants, the difference spectra obtained at different Fd concentrations allowed the determination of the dissociation constants and binding energies for the corresponding complexes (Fig. 2F and Table III). Thus, whereas L76A, L76V, L76F, L78V, L78S, V136A, V136L, and V136S exhibited K_d and ΔG^0 values similar to those of the WT enzyme, slightly weaker complexes are apparently formed by L76S, L78A, L76F/L78F, and in particular L78F, whose K_d value increased 7.5-fold relative to WT. A slight decrease of the $\Delta\epsilon$ values is also observed for L76S, L78S, L76F/L78F, and V136S. Finally, differences are also observed in the relative intensities of the bands around 394 and 462 nm in the difference spectra obtained for complexes of L78F and L76F/L78F FNR_{ox} with Fd_{ox} relative to the WT and the other FNR mutants

(Fig. 2, D and E). These effects might indicate a slightly different flavin environment in the complexes of these mutants with Fd.

Reduction of FNR Mutants Studied by Laser Flash Photolysis—The reduction of all the mutants by laser-generated dRfH[•] was monitored by the absorbance increase at 600 nm, due to FNR_{sq} formation (where sq is semiquinone). Transients were fit by monoexponential curves, and the obtained rate constants were within a factor of 2 of that of the WT FNR protein (Table IV). Table IV also shows the values of K_d for the intermediate Fd_{rd}·FNR_{ox} complex and of k_{et} , which were obtained by fitting the flash photolysis kinetic data (47, 48) for the ET transfer process between Fd_{rd} and FNR_{ox} for those mutants having non-linear FNR concentration dependencies. Second-order rate constants for the Fd_{rd}/FNR_{ox} interaction for those mutants that showed a linear FNR concentration dependence for k_{obs} are also given in Table IV.

Fig. 3A shows the dependence of k_{obs} on FNR concentration for the ET interaction between Fd_{rd} and FNR_{ox} at 100 mM ionic strength (μ) for the L76D, L78D, and L76D/L78D FNR mutants compared with WT FNR. As is evident, L78D is substantially hindered in this ET interaction and showed saturation kinetics from which a k_{et} value of $2000 \pm 200 s^{-1}$ was obtained (Fig. 3A; Table IV). The comparable value for WT FNR was $6200 \pm 400 s^{-1}$ (Table IV (7)). The value of the K_d for the intermediate Fd_{rd}·FNR_{ox} complex was about a factor of 2 larger than for WT FNR (Table IV). L76D showed a linear dependence of k_{obs} on FNR concentration, but the k_{obs} values were significantly smaller than those obtained for L78D over the entire concentration range investigated (Fig. 3A). The L76D/L78D double mutant was very impaired in its interaction with Fd_{rd}, reaching a k_{obs} value of only $15 s^{-1}$ at $65 \mu\text{M}$ FNR and $\mu = 100 \text{ mM}$ (inset in Fig. 3A). The dependence of k_{obs} on FNR concentration for this double mutant was also linear. The linearity of the concentration dependence of k_{obs} for L76D and the double mutant indicates that either there is no complex formation during the ET process or that the K_d value for the intermediate complex for these mutants is so large that protein concentrations were not reached in the accessible concentration range that would allow curvature to be observed. Note that the magnitude of impairment of the ET interaction due to substitution of a negative charge at these positions is more than additive in the L76D/L78D double mutant compared with the single mutants. Furthermore, binding of the oxidized forms of these D mutants

FIG. 2. Spectroscopic characterization of the complexes formed between selected FNR_{ox} mutants and Fd_{ox}. Difference absorption spectra are shown resulting from the addition of Fd_{ox} to WT FNR_{ox} (39 μM) (A), V136A FNR_{ox} (19 μM) (B), L76F FNR_{ox} (20 μM) (C), L78F FNR_{ox} (21 μM) (D), and L76F/L78F FNR_{ox} (23 μM) (E). The spectra were recorded at 25 °C in 50 mM Tris/HCl, pH 8.0. F, spectrophotometric titration (ΔA at 462 nm) of the following selected FNR forms with Fd_{ox}/WT FNR (×), V136A FNR (○), L76F FNR (●), L78F (□), and L76F/L78F FNR (■) (for this mutant ΔA at 390 nm is represented).

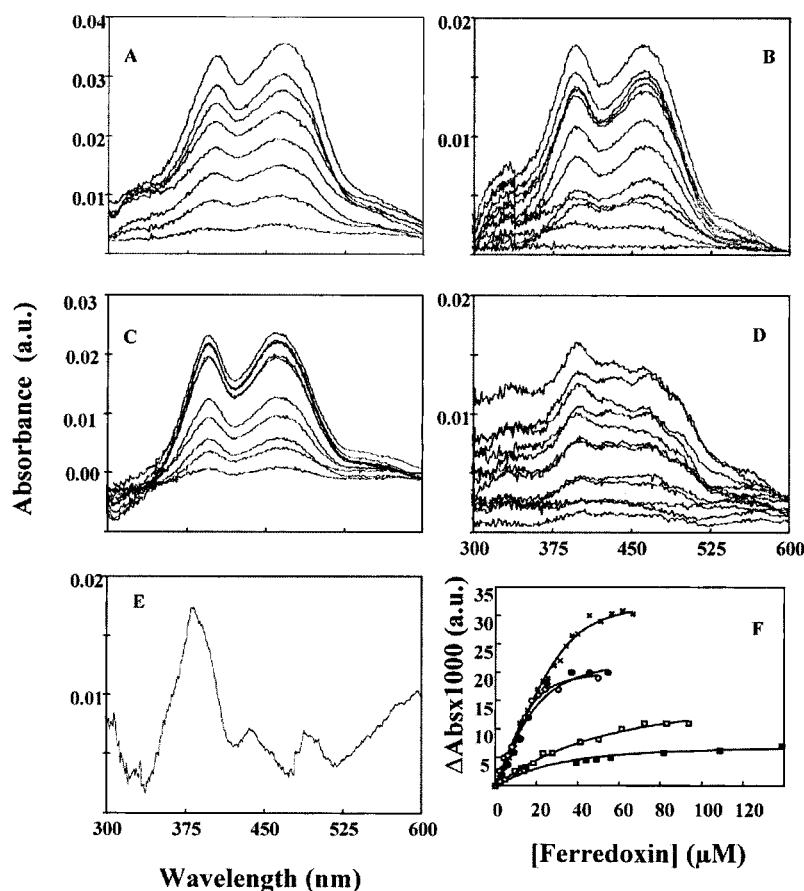


TABLE IV

Kinetic parameters for the reduction of the different FNR forms by 5-deazariboflavin and by ferredoxin as studied by laser flash photolysis

Deaerated solutions also contained 100 μM 5-dRf and 1 mM EDTA in 4 mM potassium phosphate buffer, pH 7.0. The ionic strength was adjusted to 100 mM using 5 M NaCl.

FNR form	Reduction by dRf	Reduction by ferredoxin		
	$k_{\text{dRf}} \times 10^{-8}$	$k_{\text{Fd}} \times 10^{-8}$	k_{et}	K_d
		$M^{-1} s^{-1}$	s^{-1}	μM
WT	2.1 ± 0.1	2.7 ± 0.4^a	6200 ± 400	9.3 ± 0.7
L76A	1.9 ± 0.2		6200 ± 400^b	9.3 ± 0.7^b
L76D	1.6 ± 0.1	0.16 ± 0.01	3700 ± 300	9.0 ± 0.7
L76V	2.4 ± 0.1		3700 ± 300	9.0 ± 0.7
L76F	2.2 ± 0.1	1.4 ± 0.2	6200 ± 400^c	9.3 ± 0.7^c
L76S	2.3 ± 0.3		8400 ± 700	12.2 ± 1.0
L78A	1.8 ± 0.2		5800 ± 500	13.0 ± 1.1
L78D	1.0 ± 0.1		2000 ± 200	18.8 ± 1.5
L78V	2.5 ± 0.2		6700 ± 800	22.0 ± 2.7
L78F	2.1 ± 0.1	0.79 ± 0.05	6700 ± 800	22.0 ± 2.7
L78S	2.2 ± 0.3		8100 ± 700	14.1 ± 1.2
L76D/L78D	0.9 ± 0.1	0.025 ± 0.0001	8100 ± 700	14.1 ± 1.2
L76F/L78F	3.7 ± 0.4	0.37 ± 0.05	8100 ± 700	14.1 ± 1.2
V136A	2.2 ± 0.2		6200 ± 400^b	9.3 ± 0.7^b
V136L	2.8 ± 0.1		6200 ± 400^b	9.3 ± 0.7^b
V136S	2.5 ± 0.1		6200 ± 400^b	9.3 ± 0.7^b

^a This second order rate constant was estimated from the initial slope of the plot of k_{obs} versus [FNR] in order to compare the reactivities of those mutants having linear dependencies of k_{obs} on [FNR].

^b The values of k_{obs} were scattered about the fit obtained using WT FNR, and for this reason, k_{et} and K_d were taken to be identical to the values determined for WT FNR.

^c The dependence of k_{obs} on [FNR] was linear, and therefore, values of k_{obs} and k_{et} could not be determined.

to Fd_{ox} was not detectable by differential absorbance measurements (Table IV). These ET reactivities observed at $\mu = 100$ mM are also reflected in the μ dependence curves of k_{obs} ob-

served for these mutants (Fig. 3B). The dependence of k_{obs} on μ is slightly biphasic for L78D (compared with WT FNR), showing a small increase in k_{obs} followed by a monotonic decrease as the value of μ is increased. Such biphasic dependences are frequently observed in this system and have been interpreted as indicating that the intermediate ET complex formed at low ionic strength is not in an optimal orientation for reaction (7). Both L76D and the double mutant did not show this biphasic effect in the ionic strength range measured. At the physiologically relevant value of $\mu = 100$ mM ($\mu^{1/2} \approx 0.3$), the single mutants are substantially hindered and the double mutant extremely hindered in their ET interactions with Fd_{rd}. Thus, placing a negatively charged residue at positions 76 or 78 in FNR dramatically impairs ET with Fd_{rd} at high ionic strength, but much less so or not at all at low ionic strength.

The k_{et} values obtained for L76A, L78A, V136A, and V136S were essentially the same as those of WT FNR, whereas the k_{et} values for L76S and L78S were somewhat larger (Table IV). Similarly, the values of K_d for the intermediate Fd_{rd}-FNR_{ox} complexes were essentially the same for all of these mutants as for WT FNR (Table IV). The μ dependence curves for the L76A, L78A, and V136A mutants are shown in Fig. 4A, where it is again seen that there are no large differences in the behavior of these proteins when compared with WT FNR. The shapes of the μ dependence curves for L76S, L78S, and V136S (Fig. 4B) are also similar to that of WT FNR, except that the value of k_{obs} does not decrease as much at low values of μ , and the maximal value of k_{obs} obtained for these mutants occurred at a slightly lower value of μ , indicating that less salt was required to allow the proteins to assume the optimal orientation for ET. In general, the shifts of the peaks to lower μ values relative to WT FNR are somewhat larger for the Ser mutants (Fig. 4B) compared with the Ala mutants (Fig. 4A). In addition, the values of

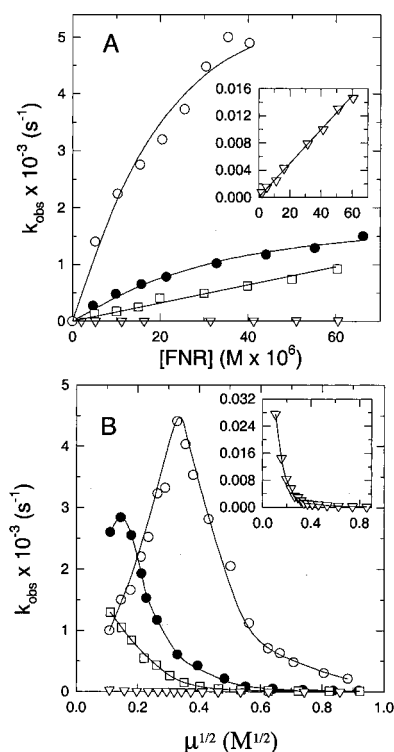


FIG. 3. *A*, FNR concentration dependence of k_{obs} for WT FNR (\circ), L78D (\bullet), L76D (\square), and L76D/L78D (∇) at $\mu = 100$ mM, obtained by laser flash photolysis. FNR was titrated into solutions containing $30 \mu\text{M}$ Fd. Solutions also contained 0.1 mM dRf and 1 mM EDTA in 4 mM potassium phosphate buffer, pH 7.0. The monitoring wavelength was 600 nm corresponding to the absorption maximum of the FAD neutral semiquinone. The ionic strength was adjusted using 5 M NaCl. *B*, ionic strength dependence of k_{obs} for WT FNR (\circ), L78D (\bullet), L76D (\square), and L76D/L78D (∇). Solutions contained $40 \mu\text{M}$ Fd and $30 \mu\text{M}$ FNR. The ionic strength was adjusted using aliquots of 5 M NaCl. Other solution conditions as in *A*. The monitoring wavelength was 600 nm.

k_{obs} at the lowest value of μ (12 mM) are three to four times larger in the case of the Ser mutants, relative to WT FNR. The FNR concentration dependence of k_{obs} for the V136S mutant was essentially identical to WT FNR at $\mu = 100$ mM (Table IV; data not shown). For this mutant, the peak in the plot of the dependence of k_{obs} value on μ is shifted to a lower value ($\mu = 30$ mM; Fig. 4B) relative to that observed for WT FNR (peak at $\mu = 110$ mM; Fig. 4B), as was also the case for the other Ser mutants.

The dependence of k_{obs} on FNR concentration at $\mu = 100$ mM for L76F, L78F and the double mutant, L76F/L78F, was linear (Fig. 5), and, therefore, values of k_{et} and K_d for the intermediate complex could not be obtained. Thus, either there is no complex formation during the ET process or the K_d value for the intermediate complex for these mutants is very large. As shown by the FNR concentration dependence of k_{obs} in Fig. 5, the reactivity of L78F was decreased by a factor of 2 or less over the FNR concentration range studied, relative to the L76F mutant. The reactivity of the L76F/L78F double mutant was decreased by about another factor of 2. Second-order rate constants obtained from these plots are reported in Table IV. For the sake of comparison, a value of $2.7 \times 10^8 \text{ M}^{-1} \text{ s}^{-1}$ can be calculated from the initial slope of the k_{obs} versus WT FNR curve at $\mu = 100$ mM (Fig. 3A and Table IV). Thus, each of these Phe mutants is significantly hindered in its ET interaction with Fd_{red}, with L76F/L78F showing the largest effect. The dependence of k_{obs} on μ for L76F, L78F, and L76F/L78F is shown in Fig. 6A, where it is seen that L76F is similar to WT FNR, although the peak value of k_{obs} is decreased somewhat (by about 20%), indicating some impairment of ET for this mutant. The peak in

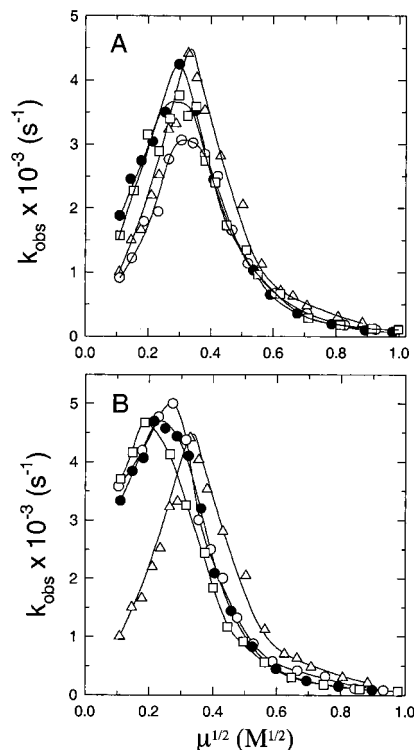


FIG. 4. Ionic strength dependence of k_{obs} obtained by laser flash photolysis for WT FNR (\triangle), L76A (\bullet), L78A (\circ), and V136A (\square) (*A*) and WT FNR (\triangle), L76S (\circ), L78S (\bullet), and V136S (\square) (*B*). Solutions contained $40 \mu\text{M}$ Fd and $30 \mu\text{M}$ FNR. The ionic strength was adjusted using aliquots of 5 M NaCl. Other conditions as in Fig. 3A. The monitoring wavelength was 600 nm.

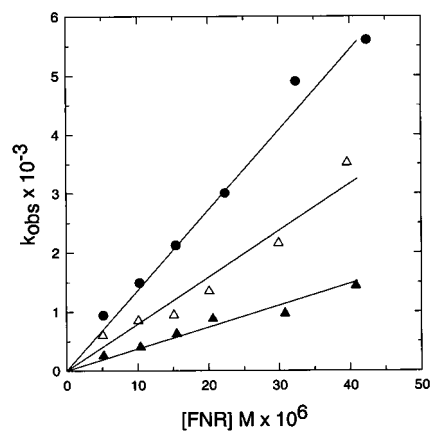


FIG. 5. FNR concentration dependence of k_{obs} obtained by laser flash photolysis for L76F (\bullet), L78F (\triangle), and L76F/L78F (\blacktriangle) at $\mu = 100$ mM. FNR was titrated into solutions containing $40 \mu\text{M}$ Fd. Other solution conditions as in Fig. 3A. The monitoring wavelength was 600 nm.

the μ dependence curve for this mutant occurs at the same value of μ as for WT FNR. L78F is impaired even more than L76F (to about 55% the WT value if the peak k_{obs} values are compared), and the peak value for k_{obs} occurs at a slightly lower value of μ . The k_{obs} value at the lowest value of μ investigated (12 mM) is about two times larger for L78F than that measured for WT FNR at this same μ value. The largest value of k_{obs} for L76F/L78F is decreased further still (to about 30% of the WT value) and does not show a peak in the range of μ investigated but only shows a monotonic decrease in k_{obs} as μ is increased. The values of k_{obs} at $\mu = 100$ mM in these plots (Fig. 6A) are consistent with the second-order rate constants calculated (Table IV) from the FNR concentration dependence plots for these

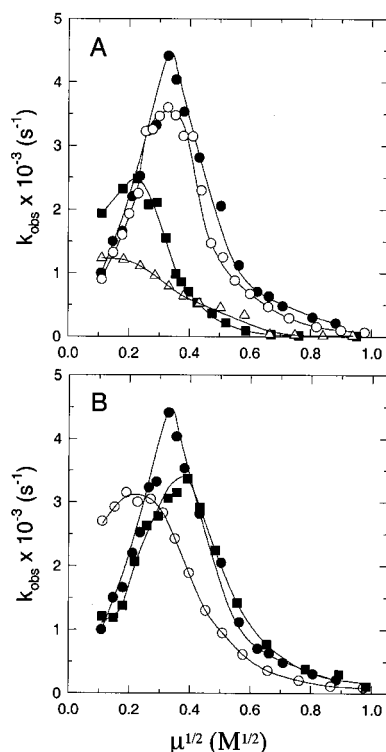


FIG. 6. Ionic strength dependence of k_{obs} obtained by laser flash photolysis for WT FNR (●), L76F (○), L78F (■), and L76F/L78F (Δ) (A) and WT FNR (●), L76V (○), and L78V (■) (B). Solutions contained 30 μM each protein except for the WT FNR and L76V experiments that contained 40 μM Fd and 30 μM FNR. The ionic strength was adjusted using aliquots of 5 M NaCl. Other solution conditions are as in Fig. 3A. The monitoring wavelength was 600 nm.

mutants shown in Fig. 5, when compared with the second-order rate constant estimated for WT FNR (Table IV).

The kinetic parameters derived from the dependence of k_{obs} on FNR concentration at $\mu = 100$ mM for L76V and L78V are given in Table IV (data not shown). The k_{et} value obtained for L78V is the same as for WT FNR, but the K_d value for the intermediate complex is two times as large as that found for WT FNR (Table IV). The k_{et} value determined for L76V is approximately one-half the value determined for WT FNR, and the K_d for the intermediate complex involving L76V is essentially identical to the value determined for the WT protein. The FNR concentration dependence of k_{obs} for V136L at $\mu = 100$ mM and the μ dependence curve were almost superimposable with those of the WT protein (data not shown).

Stopped-flow Studies of the Reduction by NADPH of Some FNR Mutants—To better understand the behaviors observed for some mutants in the steady-state diaphorase assay, the reduction by NADPH was also analyzed by stopped-flow methodologies as reported previously (14). The biphasic decrease in absorption observed at 460 nm was reported to be due to the rapid formation of a charge transfer complex, $[\text{FNR}_{\text{ox}}\text{-NADPH}]$, followed by hydride transfer from NADPH to FAD. When analyzing this reaction for the L76A, L76D, L78D, L76F/L78F, L76D/L78D, V136A, and V136L FNR mutants, the same biexponential behavior reported for the WT was observed (Table V, data not shown). For each of these mutants charge transfer complex formation occurred almost entirely within the dead time of the instrument, as was the case for WT FNR. Moreover, the introduction of negative charges at positions 76 and/or 78, Ala at positions 76 or 136, Leu at position 76, or Phe at positions 76 and 78 did not affect the hydride transfer reaction. Therefore, this might indicate that the decrease observed for the k_{cat} values in the diaphorase assay upon introduction of

TABLE V

Fast kinetic parameters for electron transfer reactions of wild-type and mutated FNR forms studied by stopped-flow

The following samples were mixed in the stopped-flow spectrometer. $T = 13$ °C. All samples were prepared in 50 mM Tris/HCl, pH 8.0.

FNR form	k_{obs} (s^{-1}) for the mixing of FNR _{ox} with		k_{obs} (s^{-1}) for the mixing of FNR _{rd} with Fd _{ox} ^c
	NADPH ^{a,b}	Fd _{rd} ^c	
WT ^d	>600	^e	^e
	>140	250 ± 30	
L76A	>600	^e	^e
	>200	260 ± 30	
L76D	>600	18 ± 5	0.026 ± 0.001
	>200	5.2 ± 0.2	
L76V		250 ± 30	200 ± 20
		40 ± 10	
L76F		>400	250 ± 50
L76S		^f	^f
L78A		^e	^e
		>220	
L78D	>600	15.2 ± 2.5	0.030 ± 0.002
	>200	2.57 ± 0.10	
L78V		^e	>600
		160 ± 30	
L78F		146 ± 15	240 ± 30
L78S		^e	0.41 ± 0.07
L76D/L78D	>600	0.10 ± 0.02	0.015 ± 0.002
	>200	0.009 ± 0.003	
L76F/L78F	>600	50 ± 8.0	1.0 ± 0.3
	>200		
V136A	>600	^e	>400
	>200	>300	
V136L	>600	^e	>350
	>200	>400	
V136S		^e	1.0 ± 0.4
		100 ± 10	

^a Reactions followed at 460 nm.

^b Most of the first reaction took place within the dead time of the instrument. Values for the observed rate constant of the second process are imprecise because of the difficulty resolving them from the first phase.

^c Reactions followed at 507 nm.

^d Data from Ref. 14.

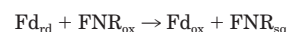
^e Reaction occurred within the dead time of the instrument.

^f No reaction was detected.

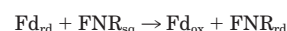
these mutations at positions 76, 78, and 136 might be due to an effect on the interaction with the DCPIP.

Stopped-flow Studies of the Reaction between Mutants of FNR and Fd—Stopped-flow kinetic studies of the FNR/Fd reaction were also carried out for the FNR mutants in order to provide additional information on the interactions between FNR and Fd. This technique not only allows one to measure the rate constant of the reaction in which reduced Fd acts as electron donor to FNR, but it also allows the measurement of the rate for the reverse reaction, *i.e.* from reduced FNR to Fd. As discussed previously, most such reactions between WT FNR and WT Fd occur within the dead time of the instrument. However, it has been shown previously that some FNR mutants show lower ET rates that can be measured using this method (14–17). As shown in Fig. 7, this is the case for some of the FNR mutants analyzed here.

As reported previously, biexponential traces are expected for the reactions between Fd_{rd} and FNR_{ox}, due to the following sequential Reactions 1 and 2,



REACTION 1



REACTION 2

In the case of the WT enzyme, the first reaction occurs within

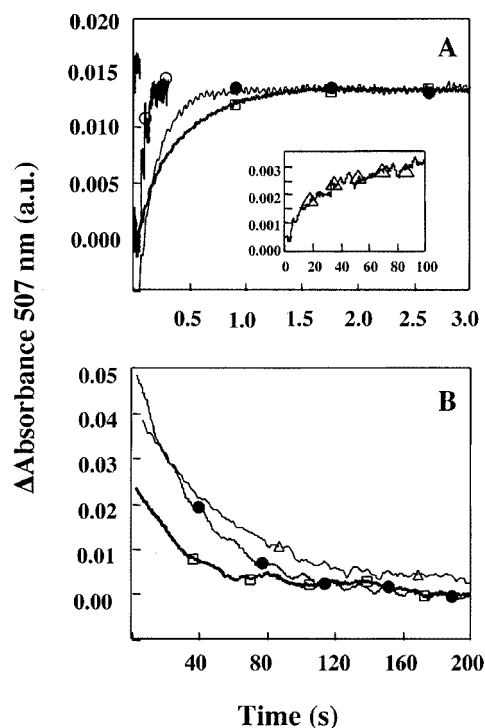


FIG. 7. Time course of the anaerobic reactions of selected FNR forms with Fd as measured by stopped-flow. Reactions were carried out in 50 mM Tris/HCl, pH 8.0, at 13 °C. The monitoring wavelength was 507 nm. Final concentrations are given in parentheses below. A, reaction of WT FNR_{ox} (8.4 μM) with Fd_{red} (26 μM) (—), V136L FNR_{ox} (9.2 μM) with Fd_{red} (25 μM) (○), L76D FNR_{ox} (8.8 μM) with Fd_{red} (17.8 μM) (●), L78D FNR_{ox} (11.6 μM) with Fd_{red} (23.2 μM) (□), and L76D/L78D FNR_{ox} (10.3 μM) with Fd_{red} (21.6 μM) (Δ). B, reaction of L76D FNR_{red} (8.6 μM) with Fd_{ox} (24.7 μM) (●), L78D FNR_{red} (7.9 μM) with Fd_{ox} (21.1 μM) (□), and L76D/L78D FNR_{red} (11.3 μM) with Fd_{ox} (24.9 μM) (Δ).

the instrumental dead time (as expected from the high k_{et} values obtained by laser flash photolysis), and only a single k_{obs} value of 250 s⁻¹, corresponding to the second process, has been detected (14–17). When analyzing these reactions for the different FNR mutants, a behavior similar to that of the WT FNR is observed for L76A, L78A, L78V, V136A, V136L, and V136S, whereas in the case of the interaction of Fd_{red} with L76V FNR both reactions can be clearly detected, having values of 250 ± 30 and 40 ± 10 s⁻¹ for the two sequential processes (Table V). It is worth noting that no reaction was detected for the reduction of L76S and L78S FNR forms by Fd_{red} under our stopped-flow experimental conditions, probably due to the fact that it took place within the instrumental dead time, as suggested by the rate constants observed in the laser flash photolysis experiments (Table IV). Replacement of Leu-76 and/or Leu-78 by Asp results in considerable impairment of the ability of FNR to accept electrons efficiently from Fd_{red}, as deduced from the very small k_{obs} values detected by stopped-flow, with the double mutant showing the largest amount of impairment (Table V). This is consistent with the flash experiments. The behavior observed for those mutants in which a Phe residue has been introduced at positions 76 and/or 78 is also noteworthy. Only a single phase, having a k_{obs} value of 400 s⁻¹, is observed for the reduction of L76F by Fd_{red}, indicating a behavior similar to the WT enzyme. Monophasic reactions are also observed for the reduction of L78F and L76F/L78F, having k_{obs} values that are 2.5 and 8 times smaller, respectively, than the L76F mutant.

Reduction of Fd by the different FNR_{red} mutants was also assayed. In all cases, the stopped-flow reactions were best fit to single exponential processes having similar amplitudes (Fig. 7B). These data have been interpreted as corresponding to the

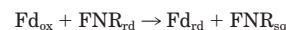
TABLE VI

Reduction potentials of the different FNR mutants

The range of experimental error was ±1–3 mV for all FNR forms examined.

FNR	E_m	$E_{mMT} - E_{mWT}$
		mV
WT	-325	
L76D	-330	-5
L76F	-333	-8
L76S	-305	+20
L78D	-302	+23
L78F	-307	+18
L78S	-286	+39
L76D/L78D	-317	+8
V136S	-305	+20

following process (Reaction 3):



REACTION 3

This process is too fast to be detected for the reduction of Fd by L76A and L78A FNR forms, as was the case for the WT FNR (14, 49). Although nearly limited by the instrumental dead time, a decay is detectable at 507 nm for the reactions of the L78V, V136A, and V136L FNR forms, demonstrating that these mutations affected the process to a small degree, whose magnitude we are not able to quantify. L76V, L76F, and L78F FNR_{red} showed rate constants for the reduction of Fd in the range of 200–250 s⁻¹, whereas a considerably smaller k_{obs} value (1.0 ± 0.3 s⁻¹) was obtained for the double mutant L76F/L78F. Introduction of Ser residues at positions 76, 78, or 136 of *Anabaena* FNR also caused an impairment of the ability of the enzyme to reduce Fd. Thus, no reaction was detected by stopped-flow methods when assaying L76S, and k_{obs} values of only 0.41 ± 0.07 and 1 ± 0.4 s⁻¹ were obtained for the reactions of L78S and V136S, respectively. Finally, very slow processes were observed when reductions of Fd by *Anabaena* FNR mutants having an Asp residue at positions 76 and/or 78 were assayed (Table V and Fig. 7B).

Flavin reoxidation of the different FNR_{red} mutants by molecular oxygen was also measured by stopped-flow spectrophotometry at 460 and 600 nm as described previously (14). Traces obtained for all the mutants (not shown) followed similar profiles to those observed for the WT enzyme, indicating that the mechanism of reoxidation of these mutants is similar to that of the native FNR, resulting in the production of an intermediate semiquinone.

Redox Potentials of FNR Mutants—The two-electron redox potential values of some of the FNR mutants at positions 76, 78, and 136 of *Anabaena* FNR have been measured. Substitution of the Leu residues at either positions 76 or 78 produced only marginal effects on the flavin redox potential (Table VI). Although introduction of an Asp or a Phe at position 76 shifted the redox potential to slightly more negative values, the other mutants analyzed had E_m values that showed moderate positive shifts relative to WT FNR. Thus, the largest shift observed, 40 mV, is due to the replacement of Leu-78 by Ser. L76S, L78D, L78F, and V136S had E_m values that were ~20 mV more positive than WT. The E_m value obtained for the double L76D/L78D mutant is intermediate between the two single mutants. Thus, these data indicate that substitutions at positions 76, 78, and 136 only slightly modulate the redox properties of the flavin ring within the protein, with the residue at position 78 having the largest influence.

Crystallographic Structures of FNR Mutants L78D, L76D/L78D, and V136L—Structure determination of the L78D,

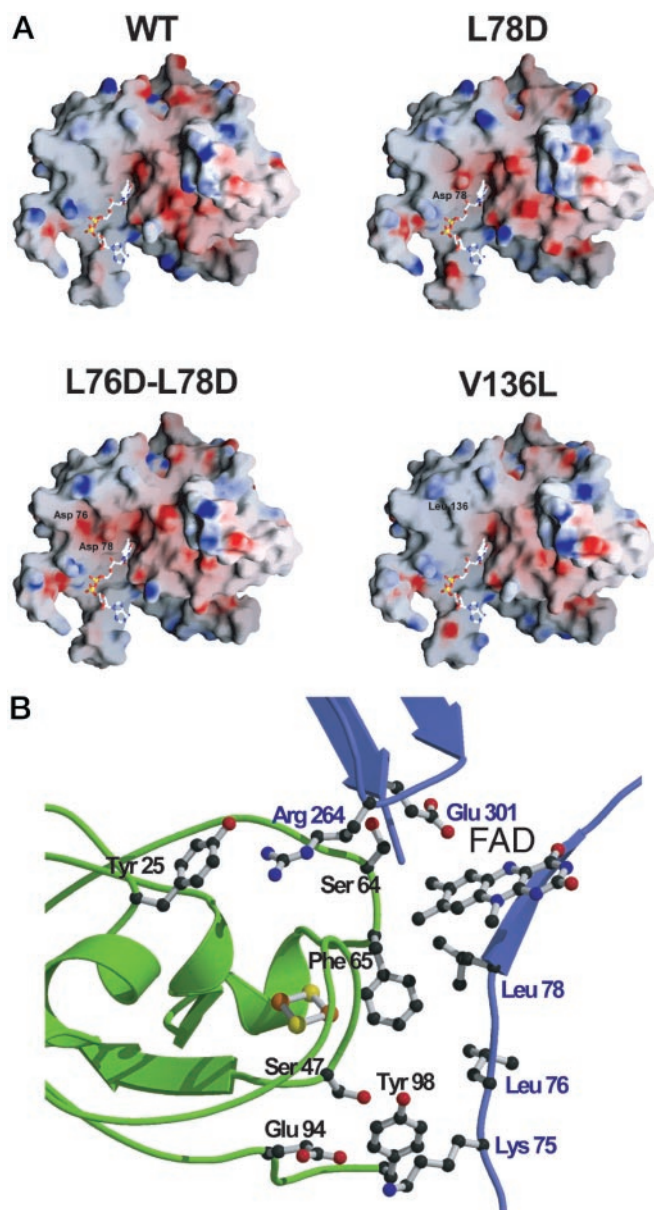


FIG. 8. *A*, molecular surface representation of FNR showing the electrostatic potential. Negative potential is represented in red and positive potential in blue. The FAD cofactor is drawn in a sticks representation. The replacement of Leu by Asp at sites 76 and 78 induces a negatively charged region, which extends over the large hydrophobic interface. This effect is markedly increased in the double mutant. In contrast, V136L mutant does not reveal any significant changes in surface potential compared with the WT, as expected. This figure was done using GRASP (55). *B*, a detailed view of the *Anabaena* FNR (blue) and Fd (green) interaction at the [2Fe-2S] cluster site including Lys-75, Leu-76, Leu-78, Arg-264, and Glu-301 FNR side chains and Tyr-25, Ser-47, Ser-64, Phe-65, Glu-94, and Tyr-98 Fd side chains. The figure was done using Molscript (54).

L76D/L78D, and V136L mutants was carried out by x-ray crystallography. In all cases the structure is essentially identical to that of the wild-type FNR. Only subtle changes are observed in the L76D/L78D mutant in the vicinity of the Asp-76 site. A slight shift of 0.5 Å is observed in the backbone, which is a consequence of two new hydrogen bonds from Asp-76 to I62(N) and to R77(N). As can be seen in Fig. 8A, the Leu → Asp replacement introduces a negatively charged region near the FAD cofactor, which is involved in the hydrophobic area of the complex interface (26). Obviously in the double mutant this effect is enlarged. On the other hand, the very conservative Val

→ Leu mutation does not disturb the hydrophobic character of the interaction with the protein partner.

DISCUSSION

The three-dimensional structure of FNR shows that the isoalloxazine ring of the FAD redox center binds at the bottom of a concave cavity to which, as indicated by all available biochemical and structural data, Fd binds during catalysis (17, 24–27). Since Fd is a one-electron carrier protein and two electrons are required by the reductase to reduce NADP⁺, it is necessary that association and subsequent dissociation of the two proteins occur at rates that are compatible with the catalytic turnover. It is in these processes of association and dissociation that electrostatic interactions have been proposed to play an important role (6, 10, 15–17). However, in the FNR/Fd system hydrophobic interactions might also be involved in such processes, as well as in the ET mechanism itself, as suggested by the important role reported for Phe-65 in *Anabaena* Fd (7, 9). In the present study three hydrophobic amino acid residues, Leu-76, Leu-78, and Val-136 (Fig. 1A), situated within the proposed Fd interaction site of the *Anabaena* FNR surface and in close proximity to the flavin ring have been replaced by a series of other residues. These three residues are fully conserved in all cyanobacterial and leaf FNR species and are replaced by Val and Ser, respectively, in those proteins from roots (Fig. 1B). Noticeably, although the region containing these residues possesses considerable structural and sequence homology to other enzymes of the FNR family, residues equivalent to Leu-76, Leu-78, and Val-136 of *Anabaena* FNR are not conserved within this family, nor are their substitutions of a conservative nature (Fig. 1B).

No significant differences were observed in the spectroscopic properties for any of the FNR mutants prepared in this study, indicating that no gross protein structural rearrangements were introduced by any of the mutations. This has been confirmed for the L78D, L76D/L78D, and V136L mutants by x-ray crystallography. The analysis of the steady-state kinetic parameters measured by the diaphorase activity indicates that, among the mutations studied here, only the introduction of a negatively charged residue at positions 76 and/or 78 or an Ala at position 136 produces enzymes that are considerably less efficient than the WT in this reaction (Table II). In contrast, measurements of the direct reduction of these mutants by NADPH using stopped-flow methodologies indicate that none of them is impaired in the processes of charge transfer complex formation or hydride transfer (Table V). Therefore, the behavior observed in the diaphorase assay for these mutants might be due to an effect on the interaction of the DCPIP with the FAD due to the introduction of a bulky residue in the vicinity of the cofactor. We conclude from these data that Leu-76, Leu-78, and Val-136 of *Anabaena* FNR are not critical residues for complex formation and ET between NADPH and FNR. This was expected since the region where NADP(H) binds to FNR is different from the area where the mutations were introduced (24, 50, 51).

In contrast to this, our results clearly indicate that the introduction of a negatively charged residue at positions 76 and/or 78 of *Anabaena* FNR impairs the ET transfer processes that take place to and from Fd (Figs. 3 and 7). Binding constants between the oxidized forms of these mutants and Fd_{ox} could not be measured, presumably because complex formation was too weak (Table III). Furthermore, in the steady-state kinetic assay, K_m values with Fd were immeasurably large for L76D and L78D, and no reaction could be detected for L76D/L78D (Table II). Moreover, although the dissociation constant obtained for the L78DFNR_{ox}-Fd_{rd} intermediate complex by flash photolysis differs only by a factor of 2 from that of the WT

enzyme (Table IV), values could not be determined for intermediate complexes involving L76D and L76D/L78D (Table IV). Differences observed in the extension of the changes observed in K_m and K_d , for example for the L78D FNR mutant, can be easily explained by taking into account the fact that K_m includes not only the dissociation of the $\text{FNR}_{\text{ox}}\cdot\text{Fd}_{\text{rd}}$ complex but also the dissociation constants for other species included in the cytochrome *c* assay, such as the $\text{FNR}_{\text{sq}}\cdot\text{Fd}_{\text{ox}}$ complex (where sq is semiquinone) and the corresponding ternary complexes with NADP^+/H . The ionic strength behavior observed for the ET from Fd to these FNR mutants suggests that the electrostatic interactions have been weakened, which results in ET-favorable interprotein orientations occurring only at lower ionic strengths (Fig. 3B). This is also indicated by the amplitudes of the fast kinetic reactions measured by stopped-flow (Fig. 7), since the reactions between the protein partners seem to occur to the same extent as with the WT enzyme, indicating that it is not the ET transfer process *per se* that is affected by the mutation, but the stabilization of the complex (Tables II–V). Again, differences in magnitudes of the changes when comparing steady state, laser flash photolysis, and stopped-flow kinetic data were also sometimes difficult to compare due to the different species produced by the special characteristics of each technique (including different protein ratios and even other compounds in the reaction mixture that are also involved in ET processes); however, an identical general tendency produced in FNR by each introduced mutation was observed. It has been shown that Arg-16, Lys-72, and Lys-75 provide a positively charged region on the FNR surface that is particularly important in the binding and orientation of Fd during ET (10, 17). Placement of a negative charge at positions 76 or 78, and especially at both positions simultaneously, produces a change of polarity in the FAD environment that must have a marked destabilizing effect on the complex (Fig. 8A). Finally, the double mutant L76D/L78D, whose activity is almost completely inhibited, has a midpoint redox potential that is quite similar to that of the WT protein (Table VI), and among these mutants only L78D has a redox potential that is significantly more positive than that of WT FNR (-302 mV *versus* -325 mV for WT). These latter results demonstrate that the effect of the mutation on the observed rates for electron exchange between the proteins is not due to an effect on the free energy of the reaction, since this parameter is determined by the difference between the midpoint redox potentials of the two proteins involved in the reaction. Thus, the drastic effect observed on the rates of reaction for these mutants is likely a consequence of a decrease in the ability of the reductase to recognize its ET protein partner due to the introduction of negative charges at these positions and, consequently, a decreased ability to form a complex that is catalytically efficient. Similar results have also been reported for other ET protein systems, such as azurin/cytochrome c_{551} and azurin/nitrite reductase, where the introduction of positively charged residues in the hydrophobic patch of azurin, which is believed to be involved in the protein-protein interaction, has been shown to impair the ET reaction (32, 52).

The L76A, L76V, L78A, L78V, V136A, and V136L FNR forms represent the most conservative substitutions of the corresponding WT side chains. Thus, the hydrophobic and non-polar character of the Leu-76, Leu-78, and Val-136 side chains are maintained, with the main difference between them being the side chain volume that extends from the protein surface. Our data indicate that all of these mutant enzymes were able to form complexes and to transfer electrons efficiently to and from Fd, as shown by the catalytic and dissociation constants obtained either by steady-state (Tables II and III) or fast kinetic (Tables IV and V) methods. However, the data also demon-

strate that the reactions are slightly modified by the introduced mutations as indicated by their interaction and kinetic parameters with Fd, which for most of these mutants are within a factor of 2 or 3 of the values determined for the WT enzyme. The most extreme case is that of the L76V FNR mutant which has rate constants, obtained either by laser flash photolysis or stopped-flow methods (Tables IV and V), that are consistently smaller than those for the WT FNR. Moreover, this mutant reaches its maximal k_{obs} value for reduction by Fd at an ionic strength value that is significantly lower than the WT enzyme (Fig. 6B). These data support the idea that FNR establishes specific hydrophobic interactions with Fd and suggests a precise hydrophobic surface complementarity at the protein-protein interface of the ET complex.

Replacement of Leu-76, Leu-78, or Val-136 by Ser, a side chain capable of forming hydrogen bond interactions, also produces some interesting effects on the ET properties of FNR. Thus, although the introduced residues apparently do not significantly affect FNR·Fd complex formation as judged by the K_d values reported here (Tables III and IV), some differences are observed in their kinetic behaviors when compared with those of the WT FNR (Tables II and IV). Laser flash photolysis data indicate that reduction of these FNR forms by Fd_{rd} is slightly faster for L76S and L78S than for the WT enzyme, with V136S being similar to WT (Table IV). On the other hand, much less efficient reactions are observed when electrons must flow in the reverse direction, from the reductase to Fd, when compared with the very fast reaction observed for the WT FNR (Tables II and V). In these three cases the introduction of a Ser side chain produces a shift of the flavin midpoint redox potential to more positive values, $+20$ mV for L76S and Val-136 FNRs and $+39$ mV for L78S (Table VI). Thus, for these mutants, the altered midpoint redox potential values are consistent with the kinetic behavior. In those reactions where electrons flow from Fd ($E_m = -384$ mV) (9) to FNR, the redox potential differences between the two reacting centers will be more favorable for the Ser mutants than for the WT enzyme. However, the opposite effect is found when electrons flow from FNR to Fd. For this latter process, structural aspects of the proteins participating in the ET processes must predominate over thermodynamic ones in the WT enzyme process, which is not thermodynamically favorable and even less so in the complex due to shifts in the reduction potential of the proteins upon complex formation (9, 53). In the case of L76S, L78S, and V136S, the thermodynamic driving force for ET from FNR to Fd is even less favorable than for the WT enzyme, and the structural arrangement around the flavin ring in the complexes between Fd and these mutants does not appear to be able to overcome effectively the non-favorable redox potential difference. Therefore, our results indicate that subtle changes in the hydrophobic FNR patch can influence the rates of ET to and from Fd by changing the binding constants, altering the midpoint redox potential of the FAD group, and changing the environment around the cofactor. Similar effects have also been reported in other protein ET systems, such as cytochrome *f* and plastocyanin, where it has also been found that the introduction of Ser residues near the heme group of the cytochrome can modulate its midpoint redox potential (31).

Also interesting is the effect observed upon replacement of either or both of the Leu residues by Phe, a hydrophobic aromatic residue whose size and rigidity is considerably greater than that of Leu. Thus, while the introduction of a Phe at position 76 produces an enzyme that can accept electrons efficiently from Fd (Fig. 6, A and B), the reactions with L78F and L76F/L78F are less efficient (Tables IV and V). The flash photolysis results indicate that either intermediate $\text{FNR}_{\text{ox}}\cdot\text{Fd}_{\text{rd}}$

functional complexes are not produced or that the K_d values are very large. Differential absorbance measurements with the oxidized proteins also indicate that slightly weaker complexes are formed and that the complexes involving L78F and especially L76F/L78F result in a somewhat different electronic arrangement around the flavin ring (Fig. 2). When reduction of Fd by these FNR mutants is measured using the cytochrome *c* reductase assay or by stopped-flow methods, it appears that the single mutants retain the ability to produce a mutual orientation of the two cofactors that can overcome the unfavorable redox potential difference (Tables II and V). However, the data indicate that the simultaneous introduction of a Phe at positions 76 and 78 disrupts the ET-favorable mutual orientation. It is noteworthy that an aromatic residue at position 65 of Fd has been proposed to be involved in the ET process. As discussed below, by taking into account the three-dimensional structure of the complex (26), the introduction of the large and aromatic Phe residues must produce a strike reorganization at the FNR/Fd interaction surface, producing a complex with an altered orientation of the two cofactors.

In summary our results confirm that although the initial interaction between FNR and Fd involves electrostatic forces between the two proteins, the overlap of the redox centers within the complex formed by these electrostatic interactions is not the most efficient for ET, probably because of an improper orientation of the two proteins (5, 7, 10, 15–17). In this context, we have also shown that non-polar residues in the region close to the FNR flavin group participate in the establishment of hydrophobic interactions between the two reactive proteins, and that these serve to orient the two redox groups in a manner such that ET is favored. It is important to note that the x-ray crystal structures recently reported for the *Anabaena* and maize FNR-Fd complexes are consistent with the results presented here (26, 27). Thus, in the *Anabaena* model, the Fd exclusively interacts with the FNR N-terminal FAD binding domain and the C-terminal structural subdomain, formed by residues 230–303. On the other hand, the NADP⁺ and its binding domain are involved to only a small extent in the FNR/Fd interaction. The model shows a remarkable shape complementarity between the concave binding zone of the reductase and the convex binding zone of the Fd (Fig. 8B). The two redox centers are very close to each other (7.6 Å, Fig. 8B), and the hydrophobic part of the isoalloxazine ring (the C-8 and C-7 methyl groups) is in direct contact with short hydrophobic side chains of Fd. The interface between Fd and FNR is stabilized by well defined hydrogen bonds, salt bridges, van der Waals interactions, and hydrophobic forces resulting from the loss of water molecules upon complex formation. The central feature of this interface consists of a compact core of hydrophobic side chains, including Phe-65 and Tyr-98 from Fd and Leu-76, Leu-78, and Val-136 from FNR and the hydrogen bond interaction of E94OE2 from Fd with K75NZ of FNR (Fig. 8B). Therefore, introduction of bulky side chains (such as a Phe at positions 76 and 78) undoubtedly modifies the arrangement of the side chains at the FNR/Fd interaction surface, and the introduction of a negative charge at positions 76 and 78 precludes Fd binding, as we have shown in this study. Thus, the major determinant of the decreased reactivity within this series of mutants can be ascribed to altered mutual orientation around the redox centers of FNR and Fd. We can conclude that formation of a complex between FNR and Fd requires the presence of certain hydrophobic amino acids residues on the surface of the reductase. These hydrophobic residues interact with Phe-65 in Fd and thereby determine the specificity of binding that is essential for the formation of a productive protein-protein complex during the electron exchange reaction.

Our data thus support the contention that the recently reported three-dimensional structure of a complex between *Anabaena* FNR and Fd could be a close representation of a functional ET transfer complex between these proteins (26).

REFERENCES

- Aliverti, A., Corrado, M. E., and Zanetti, G. (1994) *FEBS Lett.* **343**, 247–250
- Jelesarow, W., De Pascalis, A. R., Koppenol, W. H., Hirasawa, M., Knaff, D. B., and Bosshard, H. R. (1993) *Eur. J. Biochem.* **216**, 57–66
- Jelesarow, I., and Bosshard, H. R. (1994) *Biochemistry* **33**, 13321–13328
- Hurley, J. K., Salamon, Z., Meyer, T. E., Fitch, J. C., Cusanovich, M. A., Markley, J. L., Cheng, H., Xia, B., Chae, Y. K., Medina, M., Gómez-Moreno, C., and Tollin, G. (1993) *Biochemistry* **32**, 9346–9354
- Hurley, J. K., Cheng, H., Xia, B., Markley, J. L., Medina, M., Gómez-Moreno, C., and Tollin, G. (1993) *J. Am. Chem. Soc.* **115**, 11698–11701
- Hurley, J. K., Medina, M., Gómez-Moreno, C., and Tollin, G. (1994) *Arch. Biochem. Biophys.* **312**, 480–486
- Hurley, J. K., Fillat, M. F., Gómez-Moreno, C., and Tollin, G. (1996) *J. Am. Chem. Soc.* **118**, 5526–5531
- Hurley, J. K., Schmeits, J. L., Genzor, C., Gómez-Moreno, C., and Tollin, G. (1996) *Arch. Biochem. Biophys.* **333**, 243–250
- Hurley, J. K., Weber-Main, A. N., Stankovich, M. T., Benning, M. M., Thoden, J. B., Vanhooke, J. L., Holden, H. M., Chae, J. K., Xia, B., Cheng, H., Markley, J. L., Martínez-Júlvez, M., Gómez-Moreno, C., Schmeits, J. L., and Tollin, G. (1997) *Biochemistry* **36**, 11100–11117
- Hurley, J. K., Hazzard, J. T., Martínez-Júlvez, M., Medina, M., Gomez-Moreno, C., and Tollin, G. (1999) *Protein Sci.* **8**, 1614–1622
- Hurley, J. K., Faro, M., Brodie, T. B., Hazzard, J. T., Medina, M., Gomez-Moreno, C., and Tollin, G. (2000) *Biochemistry* **39**, 13695–13702
- Medina, M., Méndez, E., and Gómez-Moreno, C. (1992) *FEBS Lett.* **298**, 25–28
- Medina, M., Méndez, E., and Gómez-Moreno, C. (1992) *Arch. Biochem. Biophys.* **299**, 281–286
- Medina, M., Martínez-Júlvez, M., Hurley, J. K., Tollin, G., and Gómez-Moreno, C. (1998) *Biochemistry* **37**, 2715–2728
- Martínez-Júlvez, M., Medina, M., Hurley, J. K., Hafezi, R., Brodie, T. B., Tollin, G., and Gómez-Moreno, C. (1998) *Biochemistry* **37**, 13604–13613
- Martínez-Júlvez, M., Hermoso, J., Hurley, J. K., Mayoral, T., Sanz-Aparicio, J., Tollin, G., Gómez-Moreno, C., and Medina, M. (1998) *Biochemistry* **37**, 17680–17691
- Martínez-Júlvez, M., Medina, M., and Gómez-Moreno, C. (1999) *J. Biol. Inorg. Chem.* **4**, 568–578
- Mayoral, T., Medina, M., Sanz-Aparicio, J., Gómez-Moreno, C., and Hermoso, J. A. (2000) *Proteins* **38**, 60–69
- Arakaki, A. K., Ceccarelli, E. A., and Carrillo, N. (1997) *FASEB J.* **11**, 133–140
- Fillat, M. F., Bakker, H. A. C., and Weisbeek, P. J. (1990) *Nucleic Acids Res.* **18**, 7161
- Alam, J., Whitaker, R. A., Krogman, D. W., and Curtis, S. E. (1986) *J. Bacteriol.* **168**, 265–271
- Böhme, H., and Haselkorn, R. (1989) *Plant Mol. Biol.* **12**, 667–672
- Morales, R., Charon, M.-H., Hudry-Clergeon, G., Petillot, Y., Norager, S., Medina, M., and Frey, M. (1999) *Biochemistry* **38**, 15764–15773
- Serre, L., Vellieux, F. M. D., Medina, M., Gómez-Moreno, C., Fontecilla-Camps, J. C., and Frey, M. (1996) *J. Mol. Biol.* **263**, 20–39
- Karplus, P. A., and Bruns, C. M. (1994) *J. Bioenerg. Biomembr.* **26**, 89–99
- Morales, R., Charon, M.-H., Kachalova, G., Serre, L., Medina, M., Gómez-Moreno, C., and Frey, M. (2000) *EMBO Reports* **1**, 271–276
- Kurisu, G., Kusunoki, M., Katoh, E., Yamazaki, T., Teshima, Y., Kimata-Arigo, Y., and Hase, T. (2001) *Nat. Struct. Biol.* **8**, 117–121
- Zanetti, G., Morelli, D., Ronchi, S., Negri, A., Aliverti, A., and Curti, B. (1988) *Biochemistry* **27**, 3753–3759
- Aliverti, A., Deng, Z., Ravasi, D., Piubelli, L., Karplus, P. A., and Zanetti, G. (1998) *J. Biol. Chem.* **273**, 34008–34015
- Ejdebäck, M., Bergkvist, A., Karlsson, B. G., and Ubbink, M. (2000) *Biochemistry* **39**, 5022–5027
- Gong, X.-S., Wen, J. Q., and Gray, J. C. (2000) *Eur. J. Biochem.* **267**, 1732–1742
- van der Kamp, M., Silvestrini, M. C., Brunori, M., van Beeumen, J., Hali, F. C., and Canters, G. W. (1990) *Eur. J. Biochem.* **194**, 109–118
- Tsai, C.-J., and Nussinov, R. (1997) *Protein Sci.* **6**, 1426–1437
- Wilson, I. A., and Stanfield, R. L. (1994) *Curr. Opin. Struct. Biol.* **4**, 857–867
- DeLano, W. L., Ullsch, M. H., de Vos, A. M., and Wells, J. A. (2000) *Science* **287**, 1279–1283
- Przywiecki, C. T., Bhattacharyya, A. K., Tollin, G., and Cusanovich, M. A. (1985) *J. Biol. Chem.* **260**, 1452–1458
- Tollin, G. (1995) *J. Bioenerg. Biomembr.* **27**, 303–309
- Stankovich, M. T. (1980) *Anal. Biochem.* **109**, 195–308
- Massey, V., and Hemmerich, P. (1978) *Biochemistry* **17**, 9–16
- Leslie, A. G. W. (1987) in *Proceedings of the CCP4 Study Weekend*, SERC Daresbury Laboratory, Warrington, UK (Helliwell, J. R., Machin, P. A., and Papiz, M. Z., eds) pp. 39–50
- Collaborative Computational Project Number 4 (1994) *Acta Crystallogr. D Biol. Crystallogr.* **50**, 760–763
- Navaza, J. (1994) *Acta Crystallogr. Sect. A* **50**, 157–163
- Castellano, E., Oliva, G., and Navaza, J. (1992) *J. Appl. Crystallogr.* **25**, 281–284
- Brünger, A. T. (1993) *X-PLOR: A System for X-ray Crystallography and NMR*, version 3.843, Yale University Press, New Haven, CT
- Jones, T. A., Zou, J. Y., Cowan, S. W., and Kjeldgaard, M. (1991) *Acta Crystallogr. Sect. A* **47**, 110–119
- Foust, G. P., Mayhew, S. G., and Massey, V. (1969) *J. Biol. Chem.* **244**, 964–970

47. Simonsen, R. P., Weber, P. C., Salemm, F. R., and Tollin, G. (1982) *Biochemistry* **21**, 6366–6375
48. Simonsen, R. P., and Tollin, G. (1983) *Biochemistry* **22**, 3008–3016
49. Batie, C. J., and Kamin, H. (1984) *J. Biol. Chem.* **259**, 11976–11985
50. Deng, Z., Aliverti, A., Zanetti, G., Arakaki, A. K., Ottado, J., Orellano, E. G., Calcaterra, N. B., Ceccarelli, E. A., Carrillo, N., and Karplus, A. (1999) *Nat. Struct. Biol.* **6**, 847–853
51. Medina, M., Luquita, A., Tejero, J., Hermoso, J., Mayoral, T., Sanz-Aparicio, J., Grever, K., and Gómez-Moreno, C. (2001) *J. Biol. Chem.* **276**, 11902–11912
52. van Pouderooyen, G., Mazumdar, S., Hunt, N. I., Hill, H. A. O., and Canters, G. W. (1994) *Eur. J. Biochem.* **222**, 583–588
53. Batie, C. J., and Kamin, H. (1981) *J. Biol. Chem.* **256**, 7756–7763
54. Kraulis, P. J. (1991) *J. Appl. Crystallogr.* **24**, 946–950
55. Nicholls, A., Sharp, K. A., and Honig, B. (1991) *Proteins Struct. Funct. Genet.* **11**, 281–376
56. Yao, Y., Tamura, T., Wada, K., Matsubara, H., and Kodo, K. (1984) *J. Biochem. (Tokyo)* **95**, 1513–1516
57. Karplus, P. A., Walsh, K. A., and Herriott, J. R. (1984) *Biochemistry* **23**, 6576–6583
58. Newman, B. J., and Gray, J. C. (1988) *Plant Mol. Biol.* **10**, 511–520
59. Bowsher, C. G., and Knight, J. S. (1996) *Plant Physiol.* **112**, 861
60. Aoki, H., Doyama, N., and Ida, S. (1994) *Plant Physiol.* **104**, 1473–1474
61. Hajirezaei, M., Krause, K. P., and Sonnewald, U. (1997) DDBJ/GenBankTM/EBI Data Bank accession number Y14032
62. Kumada, H. O., Aoki, H., Doyama, N., and Ida, S. (1998) *Plant Physiol.* **116**, 1192
63. Porter, T. D., and Kasper, C. B. (1985) *Proc. Natl. Acad. Sci. U. S. A.* **82**, 973–977
64. Hall, A. V., Antoniou, H., Wang, Y., Cheung, A. H., Arbus, A. M., Olson, S. L., Lu, W. C., Kau, C. L., and Marsden, P. A. (1994) *J. Biol. Chem.* **269**, 33082–33090
65. Ostrowski, J., Barber, M. J., Rueger, D. C., Miller, B. E., Siegel, L. M., and Kredich, N. M. (1989) *J. Biol. Chem.* **264**, 15796–15808
66. Hyde, G. E., and Campbell, W. H. (1990) *Biochem. Biophys. Res. Commun.* **168**, 1285–1291
67. Long, D. M., Oaks, A., and Rothstein, S. J. (1992) *Physiol. Plant.* **85**, 561–566
68. Yubisui, T., Miyata, T., Iwanaga, S., Tamura, M., Yoshida, S., Takeshita, M., and Nakajima, H. (1984) *J. Biochem. (Tokyo)* **96**, 579–582
69. Nishida, H., Inaka, K., Yamanaka, M., Kaida, S., Kobayashi, K., and Miki, K. (1995) *Biochemistry* **34**, 2763–2767
70. Correll, C. C., Batie, C. J., Ballou, D. P., and Ludwig, M. L. (1992) *Science* **258**, 1604–1610